Planta (1996) 199: 425–432

Planta

Secondary plasmodesmata formation in the minor-vein phloem of *Cucumis melo* L. and *Cucurbita pepo* L.

Gayle M. Volk[1], Robert Turgeon[1], Dwight U. Beebe[2]

[1] Section of Plant Biology, Cornell University, Ithaca, NY 14853, USA
[2] Institut de Recherche en Biologie Végétale, Université de Montréal, 4101 Rue Sherbrooke Est, Montréal, Québec H1X 2B2, Canada

Received: 15 October 1995/Accepted: 21 November 1995

Abstract. Numerous branched plasmodesmata (pd) are present between bundle-sheath cells (BSCs) and specialized companion cells known as intermediary cells (ICs) in the minor-vein phloem of melon (*Cucumis melo* L.) and squash (*Cucurbita pepo* L.). These pd were found to be secondary, i.e., they form across existing walls. Sink, sink-source transition, and source tissues were sampled from developing and mature leaves. In sink tissue, IC precursors divide to produce the two to four ICs and associated sieve elements which are present by the time of the sink-source transition. Plasmodesmata along the interface between the IC precursor and adjacent BSCs in sink tissue are unbranched and few in number. Before the leaf tissue undergoes the sink-source transition, the number of pd channels (individual branches of pd) becomes more numerous. This increase in number of pd channels occurs at least in part and perhaps entirely by branching, resulting in more channels on the IC-side than on the BSC-side. In melon there is a 12-fold increase in the number of pd channels within the IC-side of the interface and a corresponding 9-fold increase in pd channels within the BSC-side. Thus, secondary pd form by the time of the sink-source transition and may be involved in phloem loading and photoassimilate export. The system described is well-defined and amenable to experimental manipulation: secondary pd form in large numbers, at a particular interface, over a short period of time, and in a highly predictable manner.

Key words: *Cucumis* – *Cucurbita* – Intermediary cell – Phloem – Plasmodesmata – Sink-source transition

Introduction

Most plasmodesmata (pd) are primary in origin, i.e., they form during cytokinesis as the primary cell wall is laid down (Lucas et al. 1993). However, it is clear that some pd are secondary, arising by an unknown mechanism across previously constructed cell walls (Ding and Lucas 1995). In higher plants, secondary pd form during normal development in leaves (Ding et al. 1992; Ding et al. 1993) and roots (Seagull 1983; Gunning 1978), between the sieve element and companion cell (Esau and Thorsch 1985), between pollen mother cells (Cheng et al. 1987), and during fusion of plant parts (Boeke 1971; Boeke 1973; van der Schoot et al. 1995). In addition, they form across graft junctions (Kollmann and Glockmann 1985, 1991; Kollmann et al. 1985), in chimeras (Binding et al. 1987; Steinberg and Kollmann 1994), between fusing protoplasts (Monzer 1991), and during parasite-host interactions (Dell et al. 1982). Secondary pd are altered during cell-to-cell spread of certain viruses between adjacent mesophyll cells (Moore et al. 1992; Lucas and Gilbertson 1994; Waigmann et al. 1994; Wolf and Lucas 1994; Ding et al. 1995). Lateral fusion of primary pd has been documented by Ding et al. (1992).

Secondary pd may form de novo through the wall, without involvement of other pd, or by branching of primary pd. De novo secondary pd formation has been studied in most detail in graft junctions (Kollmann and Glockmann 1991) and in fusing protoplasts (Monzer 1991). The phenomenon is not as well documented during the course of normal development, although Seagull (1983) noted that pd become more clustered in root cells as they expand and postulated that de novo secondary pd are formed in association with those already in existence. Also, in *Chara*, unbranched secondary pd form by 'evagination' of the plasma membrane through a newly formed wall; these pd can then branch (Franceschi et al. 1994).

Highly branched pd have been identified between intermediary cells (ICs) and bundle-sheath cells (BSCs) in minor-vein abaxial phloem of dicotyledonous species that translocate large amounts of raffinose and stachyose

Abbreviations: BSC = bundle-sheath cell; DAP = days after planting; IC = intermediary cell; LPI = leaf plastochron index; pd = plasmodesmata; PI = plastochron interval

Correspondence to: G.M. Volk; FAX: 1 (607) 255 5407; Tel.: 1 (607) 255 8479; E-mail: gmv1@cornell.edu

(Grusak et al. 1996). Intermediary cells are specialized companion cells. They have been most thoroughly described in cucurbits (Turgeon et al. 1975; Schmitz et al. 1987; Gamalei et al. 1994), *Coleus blumei* (Fisher 1986; Gamalei et al. 1994), and several genera of the Scrophulariaceae (Turgeon et al. 1993). Intermediary cells always abut BSCs and are oriented in a lateral, peripheral position within the vein (Fig. 1). It is thought that photoassimilate is loaded symplasmically through the pd from the bundle-sheath into ICs (Grusak et al. 1996). Since loading occurs only after the developmental transition of leaf tissue from sink to source status (Turgeon 1989), we hypothesized that these structurally specialized pd are produced specifically in preparation for their role in translocation. If so, they would be formed across already-existing walls, i.e., they would be secondary in origin.

Materials and methods

Plant material. Early prolific straightneck squash (*Cucurbita pepo* L. var. *melopepo* cv. torticollis) seeds were obtained from Burpee Seed Co. (Warminster, Pa., USA) and plants were grown in soil in a controlled-environment chamber with an 18 h/4 h light/dark photoperiod, 23 °C/18 °C light/dark temperatures, and ambient relative humidity.

Melon plants (*Cucumis melo* cv. Hale's Best Jumbo, Burpee/Ball Seed Co., West Chicago, Ill., USA) were grown individually in 15-cm-diameter clay pots containing Cornell mix (Boodley and Sheldrake 1977) in a CEL 37–14 growth chamber (Sherer-Gillette/Revco/Lindberg, Asheville, N.C., USA) with a 16 h/8 h light/dark photoperiod under 160 W VHO cool-white fluorescent lamps (425 $\mu mol \cdot m^{-2} \cdot s^{-1}$) (Osram Sylvania, Inc, Danvers, Mass., USA). Light/dark temperatures were 27 °C/22 °C. After germination, pots were watered to drainage twice daily with Peters 15:5:15 Excel fertilizer solution (0.674 $g \cdot L^{-1}$, Scotts-Sierra Horticultural Products Company, Marysville, Ohio, USA). Plants were given additional fertilizer (0.6 $g \cdot pot^{-1}$) every 4 d.

Sampling locations. The plastochron interval (PI) previously determined for squash (Turgeon and Webb 1973) was verified for the described growth conditions, using 30 mm as the reference petiole length. The developmental age of a particular leaf is expressed by the leaf plastochron index (LPI), which is calculated by subtracting the serial number of the leaf from the PI (Erickson and Michelini 1957). For example, when the petiole of leaf 6, counting upwards from the first foliage leaf above the cotyledons, is 30 mm long, the PI is 6 and the LPI of leaf 6 is zero. Leaves 5 and 7 would then have LPI's of 1 and −1, respectively. The sink-source transition for squash leaves is basipetal and occurs between LPI 0.3 and LPI 1.3 under the conditions described in Turgeon and Webb (1973). Lamina pieces were sampled from apical, median, and basal intercostal regions of six squash leaves at developmental stages ranging from LPI −0.05 to 1.5. Melon leaf development is very similar to squash, and LPIs are comparable between the two species when using the same reference petiole length. The sixth leaf of melon was sampled 21 days after planting (DAP) when the lamina was between 3.7 and 4.2 cm long, as measured along the midrib (LPI 0.5). On this leaf, the sink-source transition is about 2.8 cm from the base of the lamina. Mature leaves (leaf 3 or 4, 12 cm long, 24–25 DAP) were selected for sampling from a melon plant grown under the same conditions.

Electron microscopy. Squash lamina pieces (2 mm^2) were fixed in 5% (v/v) glutaraldehyde, 2 mM $CaCl_2$, in 50 mM Pipes (1,4-piperazinediethanesulfonic acid-NaOH), pH 7.4, at 4 °C for 3 h. Fixed tissues were then washed in buffer and post-fixed overnight at 4 °C in 2% (w/v) OsO_4 in the same buffer (pH 6.8). Following post-fixation, tissues were washed in buffer, dehydrated in a cold ethanol series, and infiltrated and embedded in Mollenhauers Epon-Araldite resin formulation (Mollenhauer 1964). Thin sections (pale gold) were cut with a diamond knife on a Reichert-Jung (Wein, Austria) Ultracut, stained with uranyl acetate and lead citrate, and viewed and photographed either at 80 kV with a JEOL (Tokyo, Japan) JEM 100S or at 75 and 50 kV with an Hitachi (Tokyo, Japan) H600 transmission electron microscope.

Immature melon leaf tissue was fixed in glutaraldehyde, post-fixed in osmium tetroxide, and stained with uranyl acetate as described by Ding et al. (1993). After dehydration in ethanol, samples were infiltrated with Epon-Araldite resin. Thin sections (70 nm) were mounted on copper grids, stained with uranyl acetate and lead citrate, and viewed and photographed at 60 kV with a Philips (Eindhoven, The Netherlands) EM-300 transmission electron microscope. Mature melon leaves were sampled from a median intercostal region of a fully expanded leaf. Samples were fixed, embedded, and observed as described by Haritatos et al. (1996).

Cryofixation. Squash leaf pieces (8 cm^2) were sampled as above from a different series of expanding leaves ranging from LPI 0.3 to 1.7 and aspirated at room temperature in 20 mM Mes (2-[N-morpholino]ethanesulfonic acid-NaOH, 20 mM $CaCl_2$, 20 mM KCl), pH 5.5, containing 200 mM sucrose. These pieces were then cut into smaller (1 mm^2) pieces, flash-frozen in a Balzers HPM 010 high-pressure freezer (Balzers Union, Liechtenstein), freeze-substituted in 0.1% (w/v) tannic acid in anhydrous acetone for 24 h at −90 °C, transferred to a fresh solution of 2% (w/v) OsO_4 plus 2% (w/v) uranyl acetate for 24 h at −20 °C, then at 4 °C overnight, then transferred to pure anhydrous acetone for 3 h at 4 °C, and finally brought to room temperature. The tissues were rinsed three times with fresh anhydrous acetone, then infiltrated and embedded in Epon-Araldite. Thin sections were cut, stained, viewed, and photographed as described above for squash.

Morphometric analysis. The term plasmodesma is used here to indicate either a single unbranched pd or a distinct interconnected complex of branched channels. The term 'pd channel' indicates an individual branch of such a complex. The frequency of pd channels was determined in melon leaf samples. Plasmodesmal channels were counted on enlarged micrographs on both sides of the common wall between BSC and IC. If a pd channel intersected the plasmalemma on the BSC-side of the wall, and traversed at least 25% of the cell wall, it was counted as a BSC pd channel; likewise for the IC pd channels on the IC-side of the interface. A branching ratio was calculated by dividing the number of IC channels by the number of BSC channels. An average pd radius was calculated from all branches, without accounting for changes in radius of individual pd channels as they join other branches and traverse the middle lamella. Plasmodesmata channel frequency was calculated according to Gunning (1978), using 70 nm section thickness and 22.5 nm as pd radius.

To calculate pd frequency, the surface area of ICs must be known. Intermediary-cell length was measured using the light microscope under 400× magnification on blind endings within paradermal sections from multiple blocks of each vein class. In melon leaves of LPI 0.5, there was a linear relationship between distance from the base of the leaf and IC length, defined by the equation:

$$y = 17.85 + 0.258x$$

where y = IC length (μm) and x = % distance from base of leaf. This equation was used to determine the length of IC at any given distance from the base of the leaf for vein samples of melon leaves (LPI 0.5).

Morphometric measurements were made with a ZIDAS digitizer board (Carl Zeiss, Thornwood, N.Y., USA) on enlarged prints. From these data, we determined both IC volume and the surface area of the walls adjoining ICs and associated BSCs. The measurements obtained from the ICs of a vein were averaged. A one-way ANOVA ($\alpha = 0.05$) and the Student-Newman-Keuls (Steel and Torrie 1980)

means separation test were performed to determine if significant differences existed between characteristics of interest.

The number of plastid and mitochondria profiles per IC cross-sectional area was calculated and divided by the mean tangent diameter of the organelle (Esau and Cronshaw 1968) to determine their numerical density (Weibel 1979).

Autoradiography. Labelling of $^{14}CO_2$ and translocation studies were performed on a subset of melon plants just prior to leaf disk removal to determine the site of the sink-source transition (Turgeon 1989). Leaf 2 or 3 was exposed to 0.074 MBq $^{14}CO_2$ for 5 min, followed by a translocation period of 3 h. Leaf 6 was then frozen, freeze-dried, and autoradiographed on X-ray film as described (Turgeon 1987).

Results

The development of IC pd was followed in two ways. In melon, leaves at one developmental stage (LPI = 0.5) were sampled at two positions along the tip-to-base axis to take advantage of the basipetal pattern of tissue development during the sink-source transition (Turgeon 1989). Thus, distal samples were more mature than those near the base of the lamina. In squash, leaves were sampled at different ages (measured by LPI) in apical, median, and basal locations. In both cases, development of pd was correlated with the sink-source transition by ^{14}C-labeled photoassimilate transport experiments (Turgeon 1989). The structural development of minor veins of *Cucurbita pepo* has been described (Turgeon and Webb 1976). For orientation, a low-magnification micrograph of a developing vein is shown in Fig. 1.

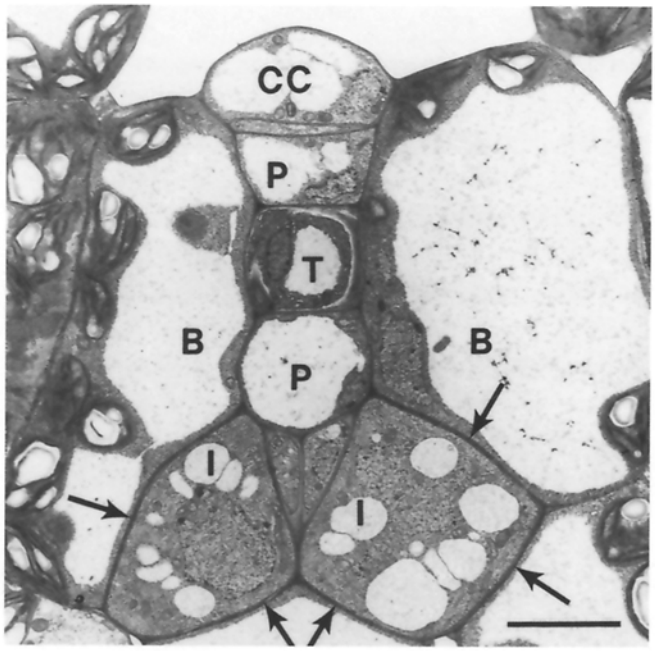

Fig. 1. Minor vein from sink-source transition region of melon leaf (LPI 0.5). Abaxial phloem contains two intermediary cells (*I*) and immature sieve elements (not labeled) adjacent to a parenchyma cell (*P*). Intermediary cells about BSCs (*B*). The IC:BSC interface is indicated by *arrows*. A developing tracheid (*T*) and adaxial companion cell (*cc*) with its immature sieve element (not labeled) are also present. Bar = 5 μm; × 3100

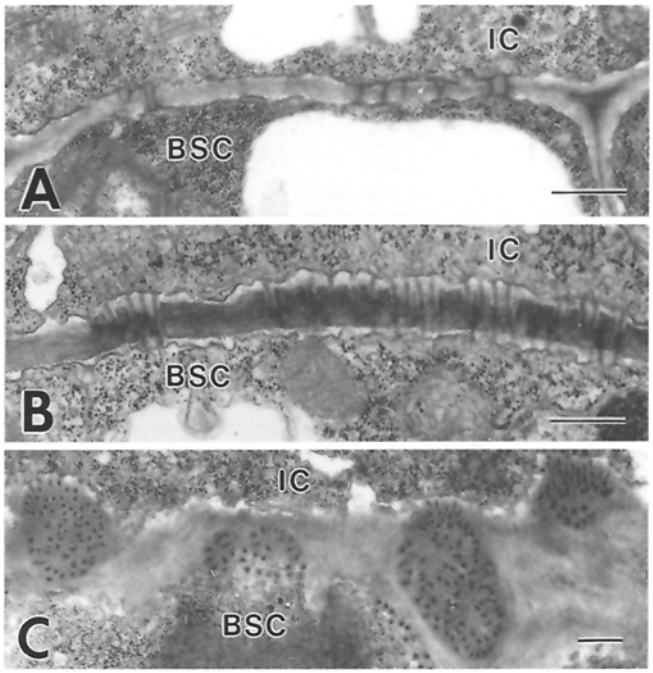

Fig. 2A–C. Ultrastructural details of pd at the IC:BSC interface of minor veins within developing *Cucurbita pepo* leaves. **A** Both unbranched and dichotomously branched pd at the IC:BSC interface of an immature minor vein from the median region of an importing leaf prior to the sink-source transition (LPI 0.2). Bar = 0.5 μm; × 20000. **B** Both unbranched and branched pd at the IC:BSC interface of a differentiating minor vein from the median region of a leaf undergoing the sink-source transition (LPI 0.9). Bar = 0.5 μm; × 20000. **C** Fields of pd at the IC:BSC interface of a structurally mature minor vein from the median region of a leaf undergoing the sink-source transition (LPI 0.9). Bar = 0.5 μm; × 12000

Sink tissue. Tissues from LPI 0.2 leaves of squash and from the basal position of LPI 0.5 melon leaves (Figs. 2A, 3A) were similar in appearance. In melon, sink tissue was sampled between 24 and 30 h before it underwent the sink-source transition. In both squash and melon, the mesophyll at this stage was compact with few intercellular spaces. Minor veins were immature, and not all sieve elements were cut off from ICs. In some cases the xylem was functionally mature, but in general all portions of the minor vein were in a developing state.

A thin cell wall separated ICs and BSCs (Table 1). Plasmodesmata along this interface were presumably primary in origin (Figs. 2A, 3A). They were evenly scattered and unbranched or occasionally dichotomously branched within the IC wall of the interface (Figs. 2A, 3A). In melon, the average radius of these pd was 22.4 ± 3.5 nm. No partial pd figures were identified in the sections observed, i.e., all pd were seen to completely traverse the wall. Table 1 lists pd frequencies and morphometric data for melon leaf tissue.

Between adjacent ICs, and between ICs and sieve elements, pd were usually unbranched (Figs. 4A, 5A). Plasmodesmata between mesophyll cells were similar to these in appearance.

Sink-source transition tissue. Leaf tissue that was just beginning to undergo the sink-source transition was

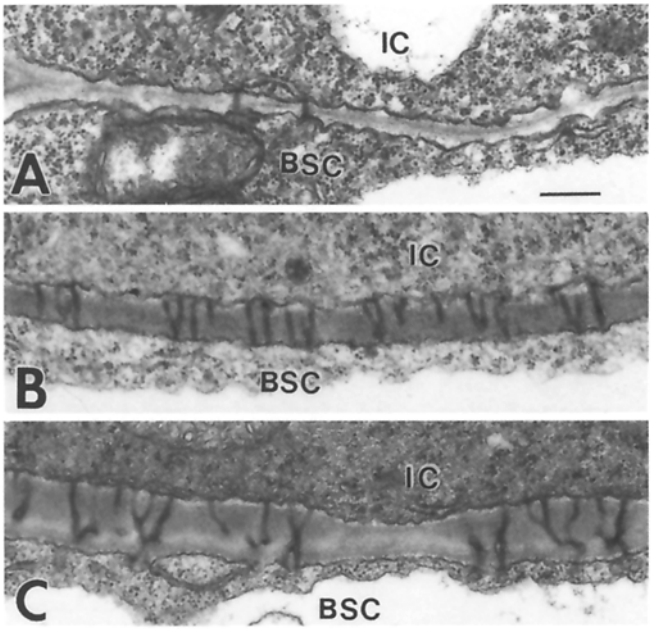

Fig. 3A–C. Plasmodesmata at the IC:BSC interface of minor veins within *Cucumis melo* leaves, representative of veins used for calculations in Table 1. **A** Unbranched pd at the IC:BSC interface in importing region (1.2 cm from base of 4 cm leaf). **B** Both unbranched and branched pd at the IC:BSC interface in the sink-source transition region of a 4 cm leaf. **C** Plasmodesmata with complex secondary branching patterns at the IC:BSC interface of a mature leaf. Bar = 0.25 μm; × 29 000

sampled 2.3 ± 0.1 cm from the base of melon leaves (LPI 0.5) or from the median region of squash leaves at LPI 0.9. Xylem was mature, with thickened cell walls and no cytoplasm. Adaxial phloem also appeared to be mature; the sieve elements had thickened cell walls and very little cytoplasm. All IC divisions were complete within the abaxial phloem, and immature sieve elements were partitioned from the ICs. There were significantly more ICs than in sink tissue (Table 1). However, these newly formed ICs did not introduce new IC:BSC wall interfaces since they were established through the formation of walls within the existing intermediary-cell precursor(s). Intermediary cells contained either several large or many small vacuoles.

Intermediary-cell plastids (0.68 μm length) were smaller than those in the BSCs (3.17 μm length) and most did not have grana, although plastoglobuli were present. The number of plastids per IC did not increase from that in the sink tissue sample. Several other IC characteristics changed, consistent with increasing cell size (length, cross-sectional area) but the most striking change was in the number of mitochondria which increased 4.5-fold between sink and sink-source transition veins (Table 1). There was no increase in plastid or mitochondria size within the ICs. Chloroplasts within bundle-sheath and mesophyll cells were mature and accumulated starch.

Plasmodesmata at the IC:BSC interface were undergoing secondary structural specialization (Figs. 2B, 3B), marked initially by an increase in branch length within the

Table 1. Comparison of characteristics among importing ($n = 6$), sink-source transition ($n = 20$), and mature ($n = 9$) veins in melon leaves. Plastid and mitochondria data, however, were collected from 6 (importing), 50 (sink-source transition), and 16 (mature) intermediary cells. Values are means ± SE. Different letters for a characteristic denote significant differences among the means of the three stages of development using the Student-Newman-Keuls means separation test after performing an ANOVA at the alpha = 0.05 confidence level. BSC, bundle-sheath cell; IC, intermediary cell; Pd, plasmodesmata; SE, sieve element; NA, not applicable

Characteristic	Sink tissue (Mean ± SE)	Sink-source tissue (Mean ± SE)	Mature tissue (Mean ± SE)
Pd along IC:BSC interface			
IC pd channels · IC^{-1}	1000 ± 500 a	12400 ± 1000 b	14300 ± 1400 b
BSC pd channels · IC^{-1}	1000 ± 500 a	9400 ± 700 b	10700 ± 1400 b
IC pd channels · μm^{-2} (IC:BSC interface)	4.3 ± 2.3 a	24 ± 2 c	14 ± 2 b
BSC pd channels · μm^{-2} (IC:BSC interface)	4.3 ± 2.3 a	18 ± 1 c	10 ± 1 b
Pd channel branching ratio	1 ± 0 a	1.3 ± 0.1 b	1.4 ± 0.1 b
Intermediary cell characteristics			
IC:BSC cell wall thickness (μm)	0.09 ± 0.01 a	0.20 ± 0.01 b	0.28 ± 0.03 c
IC:SE cell wall thickness (μm)	NA	220 ± 20 a	360 ± 25 b
Length of IC:BSC interface · IC^{-1} (μm)	10.2 ± 1.0 a	15.4 ± 1.0 b	18.7 ± 1.7 b
IC cross-sectional area (μm^2)	20.8 ± 2.0 a	34.5 ± 2.8 b	60.3 ± 5.5 c
IC length (μm)	25.2 ± 0.5 a	32.9 ± 0.5 b	59 ± 0.1 c
IC volume (μm^3)	520 ± 60 a	1120 ± 90 b	3550 ± 320 c
Number of IC · $vein^{-1}$	1.7 ± 0.2 a	2.6 ± 0.1 b	2.7 ± 0.3 b
Plastids · IC^{-1}	44 ± 20.5 a	52 ± 9.3 a	57 ± 20 a
Mitochondria · IC^{-1}	123 ± 60 a	554 ± 37 b	978 ± 115 c
IC plastid length (μm)	0.75 ± 0.09 a	0.68 ± 0.06 a	0.71 ± 0.18 a
IC mitochondria length (μm)	0.72 ± 0.05 a	0.59 ± 0.02 a	0.78 ± 0.03 a
Bundle-sheath cell characteristics			
Plastid length (μm)	2.36 ± 0.12 a	3.17 ± 0.13 b	5.44 ± 0.28 c
Mitochondria length (μm)	0.63 ± 0.10 a	0.60 ± 0.04 a	0.83 ± 0.08 a

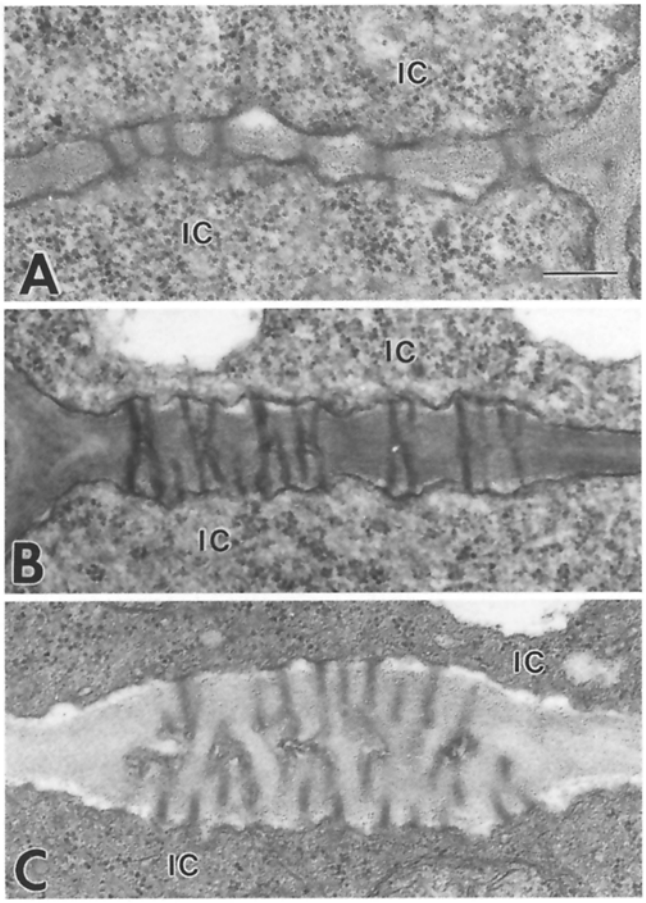

Fig. 4A–C. Plasmodesmata at the interface between contiguous intermediary cells (*IC*) of minor veins within developing leaves. **A** Unbranched pd in an unthickened portion of the common wall between two ICs from the median region of an importing leaf of *Cucurbita pepo* (LPI 0.2). **B** Plasmodesmata between two ICs within the sink-source transition region of a *Cucumis melo* leaf (LPI 0.5) **C** Complex assembly of pd in a significantly thickened portion of the common wall between two ICs from the non-importing, apical region of a leaf nearing the completion of the sink-source transition (LPI 1.2). Bar = 0.25 μm; × 40 000

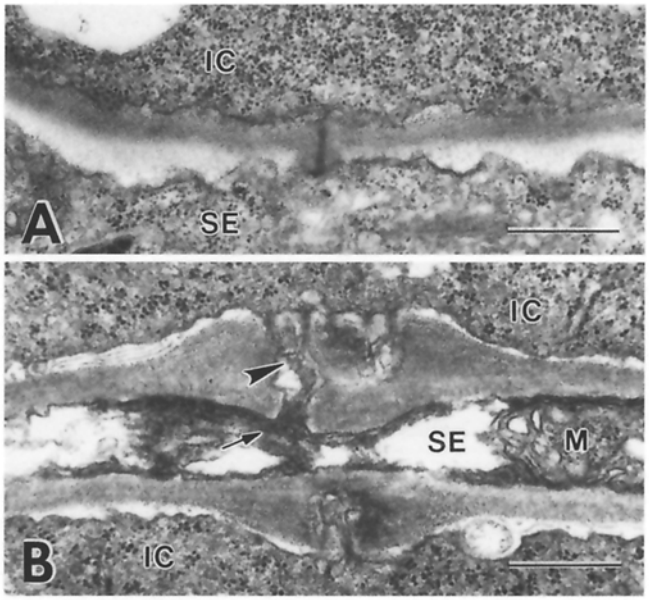

Fig. 5A, B. Intercellular connections between intermediary cells (*IC*) and sieve elements (*SE*) of minor veins within developing *Cucurbita pepo* leaves. **A** An unbranched plasmodesma lacking a median cavity between a differentiating SE and an IC within an immature minor vein from the median region of an importing squash leaf (LPI 0.2). **B** Complex pore-plasmodesmata connections between a sieve element and two contiguous ICs within a minor vein from the non-importing, apical region of a leaf undergoing the sink-source transition (LPI 1.0). Note the fusion (*arrowhead*) of the two IC desmotubules within the median cavity to form a larger, dilated central structure in the SE wall portion of the interface. *Arrow* indicates parietal array of smooth endoplasmic reticulum associated with the pore-plasmodesmata complex. *M*, mitochondrion. Bar = 0.5 μm; × 30 000

IC-side of the interface as the IC wall underwent localized thickening. Partial pd figures (believed to be due to sectioning) are present in micrographs. Plasmodesmata were branched on both the IC- and BSC-sides, but unequal branching led to an overall branching ratio of 1.3 ± 0.1 in melon (Table 1). The number of pd channels per IC in melon was 9.4-fold and 12.4-fold higher for the BSC-side and IC-side of the interfacing wall, respectively, than in sink tissue.

The wall between adjacent ICs became evenly thickened on both sides of the interface (Fig. 4B). Plasmodesmata developed distinct median cavities in which the normally compressed strand of endoplasmic reticulum forming the desmotubule became dilated and a lumen was visible. The desmotubule was difficult to observe in an extended length of the branches near the pd orifice on both sides of the interface.

Mature tissue. In melon, ICs were rounded in transverse views with a volume 3.2 times larger than that in sink-source transition tissue. The cells in the rest of the vein did not increase in size proportionately. As in immature tissue, the cytoplasm of the ICs was dense and contained many small vacuoles.

There was an average of 57 plastids per IC, not significantly more than that observed in more immature tissues. In contrast, there were 7.9-fold more mitochondria than in sink tissue ICs, and 1.8-fold more than in sink-source transition tissue ICs (Table 1). There was no significant increase in IC plastid or mitochondria length across the three developmental stages compared. However, plastids were significantly smaller in ICs than in adjacent mesophyll cells at all stages of development.

In mature tissue, the pd along the IC:BSC interfacing wall were branched (Fig. 3C). In addition, this wall increased to a thickness approximately 3 times greater on the IC-side than on the BSC-side of the middle lamella. There was also considerable change in the spatial distribution of pd by this stage of the sink-source transition: pd were clustered in fields (Fig. 2C) rather than scattered along the IC:BSC interface.

Interestingly, at the IC:sieve element interface the branches of the pd within the IC wall appeared to be much wider than those within the other two interfaces just described (compare Figs. 3C and 5B). The desmotubule was visible from the cytoplasmic orifice to the median

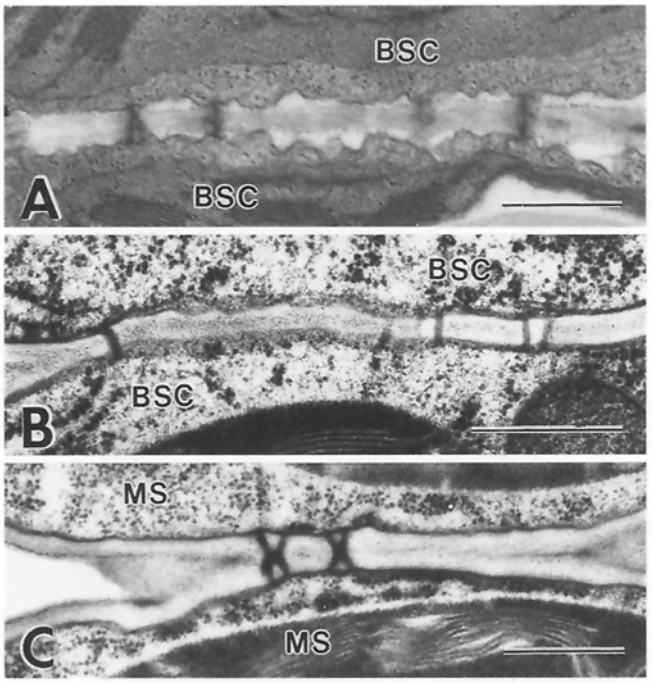

Fig. 6A, B. Structure of plasmodesmata at BSC:BSC and mesophyll cell:mesophyll cell interfaces from chemically-fixed (**A**) and cryo-fixed (**B, C**) *Cucurbita pepo* leaf tissue. **A** Both unbranched and dichotomously branched pd between bundle-sheath cells (*BSC*) from the non-importing, apical region of a leaf that has almost completed the sink-source transition (LPI 1.2). Bar = 0.5 μm; × 32000. **B** Unbranched pd between BSCs from the non-importing, median region of a leaf that has completed the sink-source transition (LPI 1.3). Bar = 0.5 μm; × 40000. **C** Evenly-branched pd between mesophyll cells (*MS*) from the median region of a leaf that has completed the sink-source transition (LPI 1.3). Bar = 0.5 μm; × 32000

region of the interface where the channel expanded significantly to form a pore within the sieve element wall. The desmotubules within the IC branches may be seen to fuse together in the large median cavity to form a larger membranous structure, which has a distinct lumen (Fig. 5B). This central membranous strand appears to be continuous with the parietal array of smooth endoplasmic reticulum within the sieve elements (Fig. 5B).

Plasmodesmata along the cell wall of adjacent BSCs were similar in appearance to those in importing veins. In both chemically-fixed (Fig. 6A) and cryo-fixed (Fig. 6B) tissue, pd between adjacent BSCs were usually unbranched or dichotomously branched. In addition, the wall surrounding the pd did not become thicker than in regions lacking pd. The distribution of pd remained scattered, without the formation of the type of pd fields seen at the IC:BSC interface (Fig. 2C). There was little change from the primary pd structure seen in pre-transition tissue (not shown). The same description is applicable to pd observed between adjacent mesophyll cells (Fig. 6C), as well as those located between BSCs and mesophyll cells.

Discussion

Secondary pd form during the maturation of ICs in developing cucurbit leaves. The timing of their formation may provide insight into the role of minor veins in these leaves. The pd present in sink tissue veins are similar in frequency, length, and appearance to that of pd positioned between mature mesophyll cells. These pd in importing veins presumably formed as the primary cell wall developed and are therefore primary in origin. However, as the tissue in a developing leaf approaches the conversion from net sink to net source, sieve elements in the minor veins approach maturity and pd between BSCs and ICs, between adjacent ICs, and between sieve elements and ICs become more complex. We hypothesize that these changes are linked to the establishment of phloem loading capacity and the initiation of assimilate export in post-transition leaves.

To avoid some of the difficulties involved with counting highly branched pd, we calculated pd channel frequencies separately along the two sides of the IC:BSC interface. Since the pd complexes in mature tissue are branched and three-dimensional, there is some bending of pd channels out of the plane of section. We calculated pd channel frequencies based upon the number of pd channels that traverse at least 25% of the wall, starting at the plasma membrane, a method that included short pd channel branches.

The pd channel frequency along the IC-side and BSC-side of the interface increased 5.6- and 4.2-fold, respectively, as the tissue matured from the sink to sink-source transition stages. Since cellular expansion was also occurring within a developing leaf, resulting in a reduction in the numbers of pd seen in thin sections, the increase in total number of pd channels is even more impressive; the values corrected for cellular expansion indicate a 12.4-fold and 9.3-fold increase in the number pd branches on the IC-side and BSC-side pd channels per IC, respectively.

Similarly, cell expansion results in an apparent decline in pd channel frequency after the sink-source transition (Table 1). However, IC length increased 1.8-fold and interface length increased 1.2-fold after the transition; with cell expansion taken into consideration, there is no statistically significant difference between the number of pd channels along the IC:BSC interface of veins in sink-source and mature regions of the leaf.

Others have taken cell expansion into account when determining overall change in pd channel frequency. Seagull (1983) determined that since a constant pd channel frequency per unit length of cell wall interface was maintained, secondary pd formation must have occurred as cellular expansion took place in the elongating root cells.

The pd channel frequencies of 10 to 14 pd channels $\cdot \mu m^{-2}$ between ICs and BSCs in mature abaxial phloem in melon were similar to those reported by Fisher (1986) in mature *Coleus blumei* veins (15.7 pd channels $\cdot \mu m^{-2}$). Coleus has ICs similar to those found in cucurbits, and it is believed to have a similar symplasmic phloem loading mechanism (Turgeon and Gowan 1992). Schmitz et al. (1987) obtained values of 50 pd channels $\cdot \mu m^{-2}$ along the same interface in mature *Cucumis melo* leaves. Since only transverse wall sections were observed in their studies, it is difficult to determine which side of the interface was used to calculate frequency data. In any case, we do not have an explanation for the discrepancies in pd channel frequencies observed.

Ding et al. (1992) found that secondary pd formation occurred by the branching of primary pd between adjacent mesophyll cells in maturing tobacco leaves after the sink-source transition was complete. The unbranched primary pd connecting adjacent mesophyll cells were modified to form structures with two or more branches on either or both sides of an enlarged central cavity. The pd along the IC:BSC interface observed in our studies appear to be structurally quite different. No enlarged central cavities were observed within the middle lamella region of a pd complex along the IC:BSC interface. Interfaces between similar cells, such as adjacent mesophyll cells or adjacent ICs, may contain cavities, although much less pronounced than those observed by Ding et al. (1993). The secondary pd formation described in our system is along an entirely different interface, one that plays a key role in phloem loading, and the general appearance of the pd along the IC:BSC interface is quite different from those described for mature tobacco mesophyll cells. The roles of pd undoubtedly differ between types of tissues and among plant species (Epel 1994).

Mature intermediary cells have plastids without grana stacks and do not accumulate starch. The IC plastids are never larger than 0.8 μm in length, significantly smaller than the chloroplasts observed in BSCs even in sink tissue. The number of plastids per IC (approximately 50) remained constant across developmental stages, despite the increase in IC volume, indicating that plastid division did not take place. This number of plastids is similar to the number of chloroplasts contained within mesophyll cells of dicotyledonous plants (20–60) (Butterfass 1979).

In contrast, the number of mitochondria per IC increased significantly between each of the three observed stages in vein development. The energy requirements for oligosaccharide synthesis are high, justifying the presence of many mitochondria in functional ICs. These mitochondria are the same size as those observed in mesophyll cells.

In the studies we have described, unbranched pd are found in veins located within importing regions of the leaf. Before veins undergo the sink-source transition there is an increase in the number of pd. As these pd form prior to the sink-source transition in developing leaves, our data support the hypothesis that pd between BSCs and ICs in cucurbits provide symplasmic channels for the transport of sugars from the mesophyll into the ICs.

We have documented the formation of secondary pd in maturing veins of cucurbits. However, further studies involving serial sections of pd fields must be conducted before it can be determined whether the branched pd observed in mature tissue are simply branches of primary pd, pd formed de novo, or a combination of both. To address this question, three-dimensional reconstruction studies of entire pd complexes are needed to determine the actual number of individual plasmodesmata. If there is an increase in the number of unbranched pd prior to the occurrence of branched pd, de novo pd formation must occur. However, it would still have to be determined whether the branched complexes observed are due to the branching of primary complexes or the formation of de novo branched complexes.

We have shown that as the minor veins in developing leaves approach the sink-source transition, numerous secondary pd form along the IC:BSC interface. The system described here is highly amenable to study and possible experimental manipulation: the pd form in large numbers, over a short time, between specific cell types, and in a highly predictable manner.

We thank Edith Haritatos, Rich Medville, Esther Gowan, and Nancy Dussault for expert technical assistance. This research was supported by an NSF/DOE/USDA Cornell Plant Science Center fellowship (G.M.V.), Natural Sciences and Engineering Research Council Grant GP0138401 and Université de Montréal, Fonds internes de recherche (D.U.B.), and NSF grant IBN-9419703 (R.T.).

References

Binding H, Witt D, Monzer J, Mordhorst G, Kollmann R (1987) Plant cell graft chimeras obtained by co-culture of isolated protoplasts. Protoplasma 141: 64–73

Boeke JH (1971) Location of the postgenital fusion in the gynocium of *Capsella bursa pastoris* (L.) Med. Acta Bot Neerl 20: 570–576

Boeke JH (1973) The postgenital fusion in the gynoecium of *Trigolium repens* L.: light and electron microscopical aspects. Acta Bot Neerl 22: 503–509

Boodley JW, Sheldrake R Jr. (1977) Cornell peat-lite mixes for commercial plant growing. NY State Coll Agric Life Sci Info Bull 43

Butterfass T (1979) Patterns of chloroplast reproduction. Springer-Verlag, New York, pp 26–27

Cheng KC, Nie XW, Chen SW, Jian LC, Sun LH, Sun DI (1987) Studies on the secondary formation of plasmodesmata between the pollen mother cells of lily before cytomixis. Acta Biol Exp Sinica 20: 1–11

Dell B, Kuo J, Burbridge AH (1982) Anatomy of *Pilostyles hamiltonii* C.A. Gardner (Rafflesiaceae) in stems of Daviesia. Aust J Bot 30: 1–9

Ding B, Lucas WJ (1996) Secondary plasmodesmata: biogenesis, special functions, and evolution. In: Smallwood M, Knox P, Bowles D (eds) Membranes: specialised functions in plant cells. BIOS Scientific Publishers, Oxford, Ltd., in press

Ding B, Haudenshield JS, Hull RJ, Wolf S, Beachy RN, Lucas WJ (1992) Secondary plasmodesmata are specific sites of localization of the tobacco mosaic virus movement protein in transgenic tobacco plants. Plant Cell 4: 915–928

Ding B, Haudenshield JS, Willmitzer L, Lucas WJ (1993) Correlation between arrested secondary plasmodesmal development and onset of accelerated leaf senescence in yeast acid invertase transgenic tobacco plants. Plant J 4: 179–189

Ding B, Li Q, Nguyen L, Palukaitis P, Lucas WJ (1995) Cucumber mosaic virus 3a protein potentiates cell-to-cell trafficking of CMV RNA in tobacco plants. Virology 207: 345–353

Epel B (1994) Plasmodesmata: composition, structure and trafficking. Plant Mol Biol 26: 1343–1356

Erickson RO, Michelini FJ (1957) The plastochron index. Am J Bot 44: 297–305

Esau K, Cronshaw J (1968) Plastids and mitochondria in the phloem of *Cucurbita*. Can J Bot 46: 877–887

Esau K, Thorsch J (1985) Sieve plate pores and plasmodesmata, the communication channels of the symplast: ultrastructural aspects and developmental relations. Am J Bot 72: 1641–1653

Fisher DG (1986) Ultrastructure, plasmodesmata frequency, and solute concentration in green areas of variegated *Coleus blumei* Benth. leaves. Planta 169: 141–152

Franceschi VR, Ding B, Lucas WJ (1994) Mechanism of plasmodesmata formation in characean algae in relation to evolution of intercellular communication in higher plants. Planta 192: 347–358

Gamalei YV, van Bel AJE, Pakhomova MV, Sjutkina AV (1994) Effects of temperature on the conformation of the endoplasmic reticulum and on starch accumulation in leaves with the symplastic minor-vein configuration. Planta 194: 443–453

Grusak MA, Beebe DU, Turgeon R (1996) Phloem loading. In: Zamski E, Schaffer A (eds) Photoassimilate distribution in plants and crops: source to sink relationships. M. Dekker, New York, in press

Gunning BES (1978) Age-related and origin-related control of the numbers of plasmodesmata in cell walls of developing *Azolla* roots. Planta 143: 181–190

Haritatos E, Turgeon R (1996) Raffinose oligosaccharide concentrations measured in individual cell and tissue types in *Cucumis melo* L. leaves: implications for phloem loading. Planta 198: 614–622

Kollmann R, Glockmann C (1985) Studies on graft unions. I. Plasmodesmata between cells of plants belonging to different unrelated taxa. Protoplasma 124: 224–235

Kollmann R, Glockmann C (1991) Studies on graft unions. III. On the mechanism of secondary formation of pd at the graft interface. Protoplasma 165: 71–85

Kollmann R, Yang S, Glockman C (1985) Studies on graft unions. II. Continuous and half pd in different regions of the graft interface. Protoplasma 126: 19–29

Lucas WJ, Gilberston RL (1994) Plasmodesmata in relation to viral movement within leaf tissues. Annu Rev Phytopathol 32: 387–411

Lucas WJ, Ding B, van der Schoot C (1993) Plasmodesmata and the supracellular nature of plants. New Phytol 125: 435–476

Mollenhauer HH (1964) Plastic embedding mixtures for use in electron microscopy. Stain Technol 39: 111

Monzer J (1991) Ultrastructure of secondary plasmodesmata formation in regenerating *Solanum nigrum*-protoplast cultures. Protoplasma 165: 86–95

Moore PJ, Fenczik CA, Deom CM, Beachy RN (1992) Developmental changes in plasmodesmata in transgenic tobacco expressing the movement protein of tobacco mosaic virus. Protoplasma 170: 115–127

Schmitz K, Cuypers B, Moll M (1987) Pathway of assimilate transfer between mesophyll cells and minor veins in leaves of *Cucumis melo* L. Planta 171: 19–29

Seagull RW (1983) Differences in the frequency and disposition of plasmodesmata resulting from root cell elongation. Planta 159: 497–504

Steel RGD, Torrie JH (1980) Principles and procedures of statistics a biometrical approach, McGraw-Hill Book Company, New York, pp 186–187

Steinberg G, Kollmann R (1994) A quantitative analysis of the interspecific plasmodesmata in the non-division walls of the plant chimera *Laburnocytisus adamii* (Poit.) Schneid. Planta 192: 75–83

Turgeon R (1987) Phloem unloading in tobacco sink leaves: insensitivity to anoxia indicates a symplastic pathway. Planta 171: 73–81

Turgeon R (1989) Sink-source transition in leaves. Annu Rev Plant Physiol Plant Mol Biol 40: 119–38

Turgeon R, Gowan E (1992) Sugar synthesis and phloem loading in *Coleus blumei* leaves. Planta 187: 388–394

Turgeon R, Webb JA (1973) Leaf development and phloem transport in *Cucurbita pepo*: Transition from import to export. Planta 113: 179–191

Turgeon R, Webb JA (1976) Leaf development and phloem transport in *Cucurbita pepo*: maturation of the minor veins. Planta 129: 265–269

Turgeon R, Beebe DU, Gowan E (1993) The intermediary cell: minor-vein anatomy and raffinose oligosaccharide synthesis in the Scrophulariaceae. Planta 191: 446–456

Turgeon R, Webb JA, Evert RF (1975) Ultrastructure of minor veins in *Cucurbita pepo* leaves. Protoplasma 83: 217–232

van der Schoot C, Dietrich MA, Storms M, Verbeke JA, Lucas WJ (1995) Establishment of a cell-to-cell communication pathway between separate carpels during gynoecium development. Planta 195: 450–455

Waigmann E, Lucas WJ, Citovsky V, Zambryski P (1994) Direct functional assay for tobacco mosaic virus cell-to-cell movement protein and identification of a domain involved in increasing plasmodesmal permeability. Proc Natl Acad Sci 91: 1433–1437

Weibel ER (1979) Stereological methods, vol. 1: Practical methods for biological morphometry. Academic Press, New York, pp 40–48

Wolf S, Lucas WJ (1994) Virus movement proteins and other molecular probes of plasmodesmal function. Plant Cell Environ 17: 573–585